

Collision Diversity SCRAM: Beyond the Sphere-Packing Bound

Sally Nafie, Joerg Robert, Albert Heuberger

Lehrstuhl für Informationstechnik mit dem Schwerpunkt Kommunikationselektronik (LIKE)

Friedrich-Alexander Universität Erlangen-Nürnberg (FAU),

91058 Erlangen, Germany

{sally.nafie, joerg.robert, albert.heuberger}@fau.de

This work has been submitted to the IEEE for possible publication. Copyright may be transferred without notice, after which this version may no longer be accessible.

Abstract—This paper presents a novel scheme dubbed Collision Diversity (CoD) SCRAM, which is provisioned to meet the challenging requirements of the future 6G, portrayed in massive connectivity, reliability, and ultra-low latency. The conventional SCRAM mechanism, which stands for Slotted Coded Random Access Multiplexing, is a hybrid decoding scheme, that jointly resolves collisions and decodes the Low Density Parity Check (LDPC) codewords, in a similar analogy to Belief Propagation (BP) decoding on a joint three-layer Tanner graph. The CoD SCRAM proposed herein tends to enhance the performance of SCRAM by adopting an information-theoretic approach that tends to maximize the attainable Spectral Efficiency. Besides, due to the analogy between the two-layer Tanner graph of classical LDPC codes, and the three-layer Tanner graph of SCRAM, the CoD SCRAM adopts the well-developed tools utilized to design powerful LDPC codes. Finally, the proposed CoD scheme tends to leverage the collisions among the users in order to induce diversity. Results show that the proposed CoD SCRAM scheme surpasses the conventional SCRAM scheme, which is superior to the state-of-the-art Non-Orthogonal Multiple Access (NOMA) schemes. Additionally, by leveraging the collisions, the CoD SCRAM tends to surpass the Sphere-Packing Bound (SPB) at the respective information block length of the underlying LDPC codes of the accommodated users.

Index Terms—Internet of Things; IoT; Internet of Everything; IoE; Machine to Machine; M2M; 6G; Low Density Parity Check Codes; LDPC; Slotted ALOHA; Coded Slotted ALOHA; Random Access; Belief Propagation; Tanner Graphs; Ultra-Reliable Low-Latency; URLLC

I. INTRODUCTION

The future systems are expected to leverage the performance enhancements which are to be delivered by 6G, in order to promote major features in diverse fields. 6G is provisioned to play a key role in Healthcare IoT (HIoT), and Industrial IoT (IIoT), in a multitude of fields such as logistics, banking, and government sectors [1], in addition to the deployment of smart sensors that perform self-diagnostics and autonomous decisions using Artificial Intelligence (AI) [2]. Moreover, 6G is expected to enhance Vehicular IoT (VIoT), by providing collaboration among connected autonomous vehicles, besides supporting Brain-Controlled Vehicles (BCV) [3]. Another prospect of the future 6G resides in the upbringing of smart cities in conjunction with the deployment of Digital Twin (DT) [4]. The realization of these use cases impose constraints on the data rate, latency, coverage, reliability, connection density, and power consumption [5].

Non-Orthogonal Multiple Access (NOMA) [6] techniques present themselves as good candidates to support the massive

connectivity constraint. In the literature, various classes of NOMA, including Power Domain (PD) and Code Domain (CD) NOMA were tackled [7]. In PD-NOMA [8], the system exploits the disparate power levels in order to differentiate between the different users. Alternatively, NOMA schemes could be designed in the code domain [9], [10]. In the literature, two powerful CD-NOMA schemes stand out; Pattern Division Multiple Access (PDMA) [11] and Sparse Code Multiple Access (SCMA) [12]. These techniques fall under the umbrella of codebook-based NOMA [13], where the analogy between Low Density Spreading (LDS) [14] and factor graph representation of codes on graphs [15] such as LDPC codes, was exploited to facilitate the Multiuser Detection (MUD).

In addition, sequence-based NOMA schemes, that rely on spreading sequences, were proposed in an attempt to optimize the tradeoff between spectral efficiency, receiver performance, and MUD complexity [16], [17]. Besides, Interleaved-based NOMA exploits the idea of uniquely designed interleavers as a candidate option to differentiate between the users [17]. Interleave Division Multiple Access (IDMA) [18] is one of the viable Interleave-based NOMA schemes.

In order to provide reliability, most of the proposed NOMA schemes rely on packet repetition or a variant thereof, which does not fully utilize the degrees of freedom. Moreover, the key terminology of the the proposed NOMA schemes depends on thoroughly coordinating the resource allocation among the users. Consequently, the proposed techniques perform poorly in terms of scalability. It is worth mentioning that in order to meet the low latency requirement, some of the aforementioned NOMA schemes propose a grant-free variant of their respective approach. However, a grant-free approach would violate the key essence of these schemes, which rely mainly on attempting to reduce the cross-correlation among the collided packets, for them to be able to resolve collisions.

The NOMA schemes presented in the literature adopt a sequential decoding scheme, portrayed in a Multiuser Detector (MUD), followed by a bank of Forward Error Correction (FEC) decoders. The MUD detector could vary between Successive Interference Cancellation [19], Belief Propagation [20], or Expectation Propagation Algorithm [21]. The output of the MUD detector is then fed to the bank of FEC decoders. Turbo-like Decoders (Iterative Detection and Decoding (IDD)) [22], involve feeding the output of the bank of the FEC decoders back to the input of the MUD detector. This could

be regarded as an iterative sequential decoding scheme.

Unlike the sequential decoders presented in the literature, a joint decoder dubbed SCRAM, which stands for Slotted Coded Random Access Multiplexing, is proposed in [23]. SCRAM combines the reliability of LDPC codes [24], with the low-latency privilege of Slotted ALOHA (SA) [25]. In a similar analogy to Belief Propagation (BP) [26] decoding of LDPC codes on a two-layer Tanner graph [27], the joint SCRAM decoder concurrently resolves collisions and decodes the LDPC codewords, on a joint three-layer Tanner graph.

In this paper, a novel approach dubbed Collision Diversity SCRAM (CoD SCRAM), that tends to further enhance the performance of SCRAM, is proposed. The essence of the CoD SCRAM scheme is threefold; First, the CoD scheme follows an information theoretic perspective in an attempt to maximize the attainable spectral efficiency. Secondly, due to the analogy between the two-layer Tanner graph of classical LDPC codes, and the three-layer Tanner graph of SCRAM, the proposed CoD SCRAM is designed such that it alleviates the detrimental factors that deteriorate the performance of classical LDPC codes. Finally, the proposed CoD SCRAM scheme leverages the collisions among the users in order to gain diversity.

The rest of this paper is organized as follows. Section II tackles the SCRAM system model, the Tanner Graph representation, and joint BP decoding. In Section III, the theoretical capacity bounds of the overloaded shared channel are derived. The design aspects of the classical LDPC Tanner graph are tackled in Section IV. Next, Section V presents the novel Collision Diversity SCRAM scheme. Then, Section VI numerically assesses the graphical structure of the proposed CoD SCRAM, revisiting the design aspects tackled in Section IV. The performance of the proposed CoD SCRAM is assessed in Section VI via Monte Carlo simulations. Finally, Section VII summarizes the paper and concludes the results.

II. SCRAM PRELIMINARIES

A. System Model

The SCRAM system incorporates N_u users sharing the SA wireless medium. Each user U_{n_u} , $\forall n_u = 1, \dots, N_u$, has an information packet, $\mathbf{b}^{(n_u)}$, of length k_{n_u} bits. This packet is encoded with an LDPC encoder, of code rate $r_{n_u} = k_{n_u}/n_{n_u}$, producing an output codeword, $\mathbf{c}^{(n_u)}$, of length n_{n_u} bits. Without loss of generality, the encoded bits are mapped to BPSK modulated symbols. The vector of modulated symbols of user U_{n_u} , is given by $\mathbf{x}^{(n_u)}$. The BPSK symbols are then transmitted using OFDM. Incorporating OFDM is twofold: to provide slot synchronization due to the gridded analogy between SA and OFDM subcarriers, and to translate the dispersive multipath fading channel to multiple flat fading subchannels. Prior to transmission, each user, U_{n_u} , randomly and independently chooses n_{n_u} SA slots (OFDM subcarriers) to transmit its modulated encoded codeword. Let N_s denote the total number of available slots per SA frame. In this case, the channel load – defined as the number of useful information bits per SA slot – is given by $D = \sum_{n_u=1}^{N_u} k_{n_u}/N_s$.

The transmitted symbols are affected by multipath fading, and perturbed by Additive White Gaussian Noise (AWGN). Due to the random selection of SA, some slots are collision free, while others suffer from collisions. The received signal

at a contended slot corresponds to the superposition of the collided faded symbols added to the AWGN.

At the receiver side, a joint decoding of the SA contended LDPC codewords is performed iteratively. The essence of SCRAM lies in the joint decoding of both SA and LDPC. Unlike the sequential decoders presented in the literature, the SCRAM mechanism incorporates a parallel three-layer Tanner graph that allows for the joint decoding. The idea is inspired by BP decoding of graph-based codes such as LDPC codes.

B. Three-Layer Tanner Graph Representation

For a SCRAM system that accommodates N_u users, the corresponding joint three-layer Tanner graph of the SCRAM decoder, comprises a set of variable nodes representing the transmitted symbols from all the users. These variable nodes are bounded by two layers of check nodes. The first check nodes layer corresponds to the slots of the shared SA medium. The other layer is driven from the conventional parity check nodes in the BP decoding of classical LDPC codes. Let N_v denote the number of variable nodes. Each transmitted symbol is represented by a variable node. Thus, $N_v = \sum_{n_u=1}^{N_u} n_{n_u}$, where n_{n_u} represents the number of transmitted symbols of user U_{n_u} per SA frame. The number of SA check nodes, denoted by N_s , is allocated according to the available radio resources. The total number of LDPC check nodes is given by $N_l = \sum_{n_u=1}^{N_u} m_{n_u}$, where $m_{n_u} \geq n_{n_u} - k_{n_u}$, denotes the number of LDPC parity check equations of user U_{n_u} .

The connections between the variable nodes and the SA check nodes rely on the random selection of the transmission slots of each user. A contended SA check node can be connected to more than one variable node. Meanwhile, the connections of the variable nodes to the LDPC check nodes are fully determined by the deployed LDPC encoder at each user's transmit terminal. This is exactly the same as the conventional representation of LDPC codes on Tanner graphs.

For illustration, consider the three-layer Tanner graph of the SCRAM model shown in Figure 1. The model incorporates $N_u = 4$ users, each transmitting $n_{n_u} = 6$ modulated symbols. For simplicity, it is assumed that the four users adopt identical LDPC encoders with $n_{n_u} = 6$ variable nodes, and $m_{n_u} = 5$ LDPC check nodes, per user. The three-layer Tanner graph of such a model consists of $N_v = 24$ variable nodes, $N_l = 20$ LDPC check nodes. Moreover, the graph has a set of $N_s = 12$ SA check nodes, that correspond to 12 allocated frequency subcarriers. Each user blindly selects six subcarriers

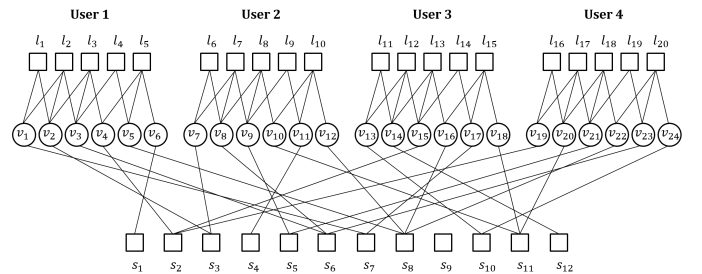


Fig. 1. Three-Layer Tanner graph example of SCRAM system with $N_u = 4$ users, each transmitting $n_{n_u} = 6$ LDPC encoded symbols over a system with $N_s = 12$ SA slots

to transmit its six modulated symbols, without prior knowledge about the selected slots of the other three users.

C. Iterative Joint SCRAM Decoding

The objective of the SCRAM decoder is to resolve the contended packets through a hybrid iterative decoding scheme, that is jointly carried out on both LDPC and SA. Inspired by Belief Propagation (BP) decoding [26] of classical LDPC codes, each decoding iteration involves two message passing steps; check nodes to variable nodes, and variable nodes to check nodes. In every iteration, the variable nodes concurrently communicate with both the SA and the LDPC check nodes, on the three-layer Tanner graph that comprises N_v variable nodes, N_s SA check nodes, and N_l LDPC check nodes.

1) *Check Nodes to Variable Nodes:* In the first half of the iteration, the SA and LDPC check nodes send their provisioned Log Likelihood Ratios (LLRs) to their corresponding variable nodes. The LLR transmitted from one check node to its corresponding variable node reflects the reliability of the transmitted value represented by this variable node.

a) *SA Check Nodes to Variable Nodes:* SA check node s_{n_s} sends an LLR to variable node v_{n_v} if they exhibit a connection in the associated three-layer Tanner graph. The LLR value S_{n_s, n_v} transmitted from SA check node s_{n_s} to variable node v_{n_v} is given by

$$S_{n_s, n_v} = \ln \frac{\sum_{\hat{m}=1}^{M_{n_s}^{(\pm)}} \left[P(y = y_{n_s} | \check{\mathbf{x}}_{\hat{m}}^{(n_v, +1)}) \cdot P(\check{\mathbf{x}}_{\hat{m}}^{(n_v, +1)}) \right]}{\sum_{\hat{m}=1}^{M_{n_s}^{(\pm)}} \left[P(y = y_{n_s} | \check{\mathbf{x}}_{\hat{m}}^{(n_v, -1)}) \cdot P(\check{\mathbf{x}}_{\hat{m}}^{(n_v, -1)}) \right]}, \quad (1)$$

where for $n_s = 1, \dots, N_s$, y_{n_s} represents the channel received signal at SA slot s_{n_s} . Let \mathcal{X}_{n_s} be the set of vectors of all the possible combinations of the collided symbols at SA check node s_{n_s} . Moreover, let $\mathcal{X}_{n_s, +1}^{(n_v)}$ and $\mathcal{X}_{n_s, -1}^{(n_v)}$ be a subset of \mathcal{X}_{n_s} that represents the set of possible vectors of all the collided symbols at SA check node s_{n_s} , that assume that the symbol represented by variable node v_{n_v} is +1 and -1, respectively. The cardinality of both $\mathcal{X}_{n_s, +1}^{(n_v)}$ and $\mathcal{X}_{n_s, -1}^{(n_v)}$, denoted by $M_{n_s}^{(\pm)}$, amounts to half the cardinality of \mathcal{X}_{n_s} . For $\hat{m} = 1, \dots, M_{n_s}^{(\pm)}$, let $\check{\mathbf{x}}_{\hat{m}}^{(n_v, +1)}$ and $\check{\mathbf{x}}_{\hat{m}}^{(n_v, -1)}$ be a vector that corresponds to one of the $M_{n_s}^{(\pm)}$ combination vectors of $\mathcal{X}_{n_s, +1}^{(n_v)}$ and $\mathcal{X}_{n_s, -1}^{(n_v)}$, respectively. Finally, $P(\check{\mathbf{x}}_{\hat{m}}^{(n_v, +1)})$ and $P(\check{\mathbf{x}}_{\hat{m}}^{(n_v, -1)})$ denote the apriori probability of the vectors $\check{\mathbf{x}}_{\hat{m}}^{(n_v, +1)}$ and $\check{\mathbf{x}}_{\hat{m}}^{(n_v, -1)}$, respectively. For $\hat{m} = 1, \dots, M_{n_s}^{(\pm)}$, the conditional probabilities of the vector $\check{\mathbf{x}}_{\hat{m}}^{(n_v, +1)} \subset \mathcal{X}_{n_s, +1}^{(n_v)}$, and the vector $\check{\mathbf{x}}_{\hat{m}}^{(n_v, -1)} \subset \mathcal{X}_{n_s, -1}^{(n_v)}$, are respectively given by

$$P(y = y_{n_s} | \check{\mathbf{x}}_{\hat{m}}^{(n_v, \pm 1)}) = \frac{1}{\pi \sigma^2} \exp \left[-\frac{\left| y_{n_s} - \sum_{d=1}^{d_{s_{n_s}}} h_{s_{n_s}, d} \check{x}_{\hat{m}, d}^{(n_v, \pm 1)} \right|^2}{\sigma^2} \right], \quad (2)$$

where $\check{x}_{\hat{m}, d}^{(n_v, +1)}$ and $\check{x}_{\hat{m}, d}^{(n_v, -1)}$ represent a possible value for the modulated symbol represented by the d^{th} variable node that collides at SA check node s_{n_s} , in the vector $\check{\mathbf{x}}_{\hat{m}}^{(n_v, +1)}$ and

$\check{\mathbf{x}}_{\hat{m}}^{(n_v, -1)}$, respectively. Moreover, $h_{s_{n_s}, d}$ denotes the estimated fading coefficient of the channel between SA check node s_{n_s} and the d^{th} variable node that collides at it. Finally, σ^2 is the noise variance of the complex AWGN channel.

At the first iteration, for $\hat{m} = 1, \dots, M_{n_s}^{(\pm)}$, the apriori probability of the vector $\check{\mathbf{x}}_{\hat{m}}^{(n_v, +1)} \subset \mathcal{X}_{n_s, +1}^{(n_v)}$, or the vector $\check{\mathbf{x}}_{\hat{m}}^{(n_v, -1)} \subset \mathcal{X}_{n_s, -1}^{(n_v)}$, is given by

$$P(\check{\mathbf{x}}_{\hat{m}}^{(n_v, +1)}) = P(\check{\mathbf{x}}_{\hat{m}}^{(n_v, -1)}) = \frac{1}{M_{n_s}^{(\pm)}}. \quad (3)$$

Starting from the second iteration, for $\hat{m} = 1, \dots, M_{n_s}^{(\pm)}$, the apriori probabilities of the vector $\check{\mathbf{x}}_{\hat{m}}^{(n_v, +1)}$, and the vector $\check{\mathbf{x}}_{\hat{m}}^{(n_v, -1)}$, are respectively given by

$$P(\check{\mathbf{x}}_{\hat{m}}^{(n_v, \pm 1)}) = \prod_{\substack{d=1 \\ v_{n_v} \neq v_{s_{n_s}, d}}}^{d_{s_{n_s}}} P(\check{x}_{\hat{m}, d}^{(n_v, \pm 1)}), \quad (4)$$

where $P(\check{x}_{\hat{m}, d}^{(n_v, \pm 1)})$ denotes the apriori probability of the d^{th} symbol, in the vector $\check{\mathbf{x}}_{\hat{m}}^{(n_v, +1)}$ and $\check{\mathbf{x}}_{\hat{m}}^{(n_v, -1)}$, respectively.

Let $V_{n_s, \hat{m}}^{(S)}$ denote the LLR that SA check node s_{n_s} , received in the previous iteration, from its corresponding variable node $v_{\hat{m}}$, such that, $v_{\hat{m}} = v_{s_{n_s}, d}$, denotes the d^{th} variable node in the set of associated variable nodes of SA check node s_{n_s} . Upon receiving these LLRs, the SA check node, s_{n_s} , updates the apriori probability of each symbol that corresponds to one of its associated variable nodes. The updated apriori probability of $\check{x}_{\hat{m}, d}^{(n_v, +1)} \in \check{\mathbf{x}}_{\hat{m}}^{(n_v, +1)}$, and $\check{x}_{\hat{m}, d}^{(n_v, -1)} \in \check{\mathbf{x}}_{\hat{m}}^{(n_v, -1)}$, are respectively calculated as follows

$$P(\check{x}_{\hat{m}, d}^{(n_v, \pm 1)}) = \begin{cases} \frac{1}{1 + \exp[-V_{n_s, \hat{m}}^{(S)}]} & \text{for } \check{x}_{\hat{m}, d}^{(n_v, \pm 1)} = +1 \\ \frac{-V_{n_s, \hat{m}}^{(S)}}{1 + \exp[-V_{n_s, \hat{m}}^{(S)}]} & \text{for } \check{x}_{\hat{m}, d}^{(n_v, \pm 1)} = -1 \end{cases}. \quad (5)$$

b) *LDPC Check Nodes to Variable Nodes:* The LLR transmitted from the LDPC check nodes to their corresponding variable nodes are calculated in the same way as the classical LDPC BP algorithm. The extrinsic information transmitted from an LDPC check node to one of its associated variable nodes represents the updated LLR of the probability of the corresponding symbol represented by the variable node, that causes the LDPC check node to be satisfied.

An LDPC check node, l_{n_l} , sends an LLR to a variable node, v_{n_v} , if and only if v_{n_v} belongs to the set of associated variable nodes of LDPC check node l_{n_l} . The LLR value, L_{n_l, n_v} , transmitted from LDPC check node l_{n_l} , to variable node v_{n_v} , is given by

$$L_{n_l, n_v} = -2 \tanh^{-1} \left(\prod_{\substack{v_{\hat{m}} \in \mathbf{V}_{l_{n_l}} \\ v_{\hat{m}} \neq v_{n_v}}} \tanh \left(-\frac{V_{n_l, \hat{m}}^{(L)}}{2} \right) \right), \quad (6)$$

where $V_{n_l, \hat{m}}^{(L)}$ represents the LLR transmitted from variable node $v_{\hat{m}}$, to LDPC check node l_{n_l} , in the previous iteration.

2) *Variable Nodes to Check Nodes:* Upon receiving the LLRs from the SA and the LDPC check nodes, the variable nodes calculate new information to be transmitted to their corresponding check nodes, both SA and LDPC, in the next half of the iteration. This information represents the LLR of their currently held symbols, based on the information they gathered from their corresponding SA and LDPC check nodes. The key essence of the joint SCRAM decoding algorithm is the simultaneous transmission of the variable nodes to both SA and LDPC check nodes.

Variable node, v_{n_v} , would send an LLR to SA check node s_{n_s} , and to LDPC check node l_{n_l} , if and only if SA check node s_{n_s} , and LDPC check node l_{n_l} , belong to the set of associated SA check nodes, and LDPC check nodes, respectively, of variable node, v_{n_v} . Let $V_{n_s, n_v}^{(S)}$ and $V_{n_l, n_v}^{(L)}$ represent the information transmitted from variable node, v_{n_v} to SA check node s_{n_s} , and LDPC check node l_{n_l} , respectively. These LLRs are respectively given by

$$V_{n_s, n_v}^{(S)} = \sum_{\substack{s_{n_s} \in \mathcal{S}_{v_{n_v}} \\ s_{n_s} \neq s_{n_s}}} S_{n_s, n_v} + \sum_{l_{n_l} \in \mathcal{L}_{v_{n_v}}} L_{n_l, n_v}, \quad (7)$$

$$V_{n_l, n_v}^{(L)} = \sum_{s_{n_s} \in \mathcal{S}_{v_{n_v}}} S_{n_s, n_v} + \sum_{\substack{l_{n_l} \in \mathcal{L}_{v_{n_v}} \\ l_{n_l} \neq l_{n_l}}} L_{n_l, n_v}, \quad (8)$$

where S_{n_s, n_v} and L_{n_l, n_v} represent the LLR, that variable node, v_{n_v} , has received in the first half of the iteration from SA check node, s_{n_s} , and LDPC check node, l_{n_l} , respectively.

III. A GLIMPSE ON INFORMATION THEORY AND THEORETICAL CAPACITY BOUNDS

A. Derivation of Collision-based Channel Capacity

1) *Random Access:* In this section, the multiuser channel capacity on the Random Access (RA) channel is derived. The adopted RA model is the Slotted ALOHA (SA) [25]. For SA, the channel is equally divided into N_s slots of equal width. These slots could either be time slots or frequency subcarriers.

Let N_u be the number of users accessing an SA frame that comprises N_s slots. Despite the fact the multiple users could collide at the same slot, the collision of two or more symbols of the same user on one SA slot is not possible [28]. This means that the number of collisions on one SA slot ranges from 0 to N_u . For $n_s = 1, \dots, N_s$, the slot degree, $d_{s_{n_s}}$, such that $0 \leq d_{s_{n_s}} \leq N_u$, is defined as the number of collided symbols (or users) at SA slot, s_{n_s} . For this model, the node degrees follow a binomial distribution [29]. This means that the probability of SA slot s_{n_s} , having a certain degree, $0 \leq d_{s_{n_s}} \leq N_u$, is given by

$$P(d_{s_{n_s}}) = \binom{N_u}{d_{s_{n_s}}} p^{d_{s_{n_s}}} (1-p)^{N_u-d_{s_{n_s}}}, \quad 0 \leq d_{s_{n_s}} \leq N_u, \quad (9)$$

where p denotes the probability that SA slot, s_{n_s} , is chosen by user, U_{n_u} .

Because of the random access, all N_s SA slots are equally-likely chosen. For $n_u = 1, \dots, N_u$, if user U_{n_u} attempts to transmit n_{n_u} symbols over an SA frame of N_s slots, the probability, p , of an arbitrary SA slot being chosen by user U_{n_u} , to transmit one of its n_{n_u} symbols is given by $p = \frac{n_{n_u}}{N_s}$.

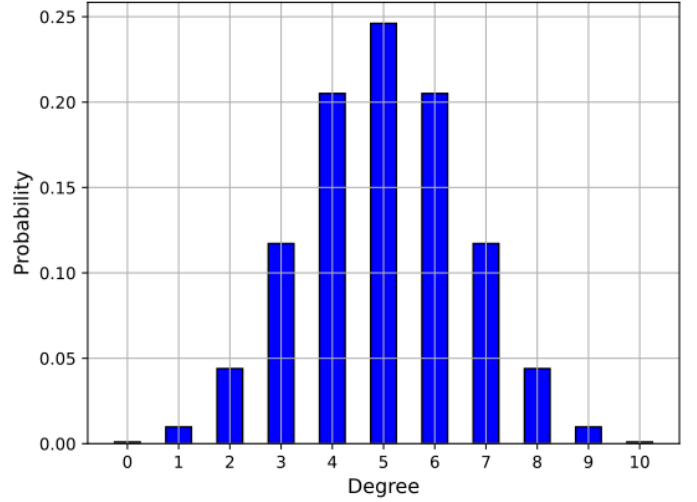


Fig. 2. Simulated degree distribution of an SA system with $N_s = 8064$ slots, incorporating $N_u = 10$ users, each transmitting $n_{n_u} = 4320$ bits

Similarly, because the users randomly choose the slots, (9) applies for all the N_s slots. Figure 2 depicts the simulated degree distribution of an SA system with $N_s = 8640$ slots, incorporating $N_u = 10$ users, where each user transmits $n_{n_u} = 4320$ bits (symbols). As shown in the figure, the degree distribution ranges from zero to ten collisions per slot. The simulated probabilities coincide with the binomial distribution of (9), computed at $p = 0.5$.

The key to deriving the capacity of this system, is to first derive the capacity of one SA slot, then extend the derivation to N_s slots. For one SA slot, the achievable sum rate, $C_{s_{n_s}}$, at SA slot s_{n_s} , is given by

$$C_{s_{n_s}} = \sum_{d_{s_{n_s}}=0}^{N_u} P(d_{s_{n_s}}) C_{d_{s_{n_s}}} \text{ bits/s/SAslot.} \quad (10)$$

Assuming each SA slot, s_{n_s} , has a bandwidth of $W_{n_s} = \frac{W}{N_s}$, the sum rate, $C_{d_{s_{n_s}}}$, corresponds to the classical single-user capacity with bandwidth W_{n_s} , and received power, $d_{s_{n_s}} \frac{P}{N_u n_{n_u}}$. Consequently, the overall sum rate, $C_{s_{n_s}}$, at SA slot s_{n_s} , in compliance with [30], can be written as

$$C_{s_{n_s}} = \sum_{d_{s_{n_s}}=0}^{N_u} P(d_{s_{n_s}}) \frac{W}{N_s} \log_2 \left(1 + \frac{d_{s_{n_s}} \frac{P}{N_u n_{n_u}}}{N_0 \frac{W}{N_s}} \right) \text{ bits/s/SAslot.} \quad (11)$$

This means that the overall sum rate, C_{SA} , of the SA system with N_s slots is given by

$$C_{SA} = N_s C_{s_{n_s}} = \sum_{d_{s_{n_s}}=0}^{N_u} P(d_{s_{n_s}}) W \log_2 \left(1 + \frac{d_{s_{n_s}} \frac{P}{N_u n_{n_u}}}{N_0 \frac{W}{N_s}} \right) \text{ bits/s.} \quad (12)$$

The total transmit power per user, $\frac{P}{N_u}$, is equivalent to $E_b R_b$, where E_b and R_b denote the energy per bit, and the transmission data rate per user, respectively. Thus, the overall sum rate can be further simplified to

$$C_{SA} = \sum_{d_{s_{n_s}}=0}^{N_u} P(d_{s_{n_s}}) W \log_2 \left(1 + \frac{E_b}{N_0} \frac{N_s d_{s_{n_s}} R_b}{n_{n_u} W} \right) \text{ bits/s.} \quad (13)$$

Moreover, the overall spectral efficiency, η_{SA} , defined as the ratio between the overall sum rate, C_{SA} , and the total bandwidth, W , is given by

$$\eta_{SA} = \sum_{d_{s_{n_s}}=0}^{N_u} P(d_{s_{n_s}}) \log_2 \left(1 + \frac{E_b}{N_0} \frac{N_s d_{s_{n_s}} R_b}{n_{n_u} W} \right) \text{ bits/s/Hz.} \quad (14)$$

Finally, substituting for $\frac{R_b}{W}$ by $\frac{\eta_{SA}}{N_u}$, the overall spectral efficiency can be written as

$$\eta_{SA} = \sum_{d_{s_{n_s}}=0}^{N_u} P(d_{s_{n_s}}) \log_2 \left(1 + \frac{E_b}{N_0} \frac{N_s d_{s_{n_s}} \eta_{SA}}{N_u n_{n_u}} \right) \text{ bits/s/Hz.} \quad (15)$$

2) *Uniform Access*: Similar to the random access channel, a multiuser uniform access channel allows for overloading. However, the uniform access imposes subtle coordination among the users, such that the number of collisions per each slot is the same.

Let the uniform multiple access channel be divided into N_s slots of equal width in the frequency domain (Mapping to time domain is straightforward). Assuming that N_u users, with n_{n_u} symbols each, attempt to share the channel, the uniform degree, $d_{s_{n_s}}$, of each slot, s_{n_s} , is given by

$$d_{s_{n_s}} = \frac{N_u n_{n_u}}{N_s}, \quad (16)$$

assuming that $\text{mod}(N_u n_{n_u}, N_s) = 0$. Mapping to the case where $\text{mod}(N_u n_{n_u}, N_s) \neq 0$ is straightforward. In that case, the overall sum rate, $C_{s_{n_s}}$, at slot s_{n_s} , can be written as

$$\begin{aligned} C_{s_{n_s}} &= \frac{W}{N_s} \log_2 \left(1 + \frac{d_{s_{n_s}} P}{N_0 \frac{W}{N_s}} \right) \\ &= \frac{W}{N_s} \log_2 \left(1 + \frac{P}{N_0 \frac{W}{N_s}} \right) \\ &= \frac{W}{N_s} \log_2 \left(1 + \frac{P}{N_0 W} \right) \text{ bits/s/slot.} \end{aligned} \quad (17)$$

Consequently, the overall sum rate of the uniform-access channel with N_s slots is given by

$$\begin{aligned} C_{uniform} &= W \log_2 \left(1 + \frac{P}{N_0 W} \right) \\ &= W \log_2 \left(1 + \frac{E_b}{N_0} N_u \frac{R_b}{W} \right) \text{ bits/s.} \end{aligned} \quad (18)$$

Thus, the overall spectral efficiency, $\eta_{uniform}$, can be written as

$$\eta_{uniform} = \log_2 \left(1 + \frac{E_b}{N_0} \eta_{uniform} \right) \text{ bits/s/Hz.} \quad (19)$$

Finally, the nominal SNR per bit, required to meet a specific target spectral efficiency, can be calculated as

$$\frac{E_b}{N_0} = \frac{2^{\eta_{uniform}} - 1}{\eta_{uniform}}. \quad (20)$$

B. Trade-off between Random Access and Uniform Access

As discussed in the previous section, a shared random access channel, that accommodates N_u users, is attributed to a binomial distribution of its channel slot degree. This means that the random access channel attains a non-zero probability of idle slots. A uniform access channel, on the other hand, although allows for collisions, maintains a uniform degree distribution to all channel slots. This means that unlike random access, unless fully idle, a uniform access channel has strictly zero probability of possessing idle slots.

For illustration, Figure 3 depicts the SA node degree distribution, obtained from a Monte Carlo simulation of a shared channel, with $N_s = 8640$ slots, adopting random access, and uniform access, for various number of users. Figures [a] through [d], show the node degree distribution of $N_u = \{2, 4, 8, 16\}$ users, respectively, with $n_{n_u} = 4320$ symbols each. As shown in the figures, for all the different number of users, the random access schemes always show a binomial behavior in their simulated degree distribution, that coincides perfectly with the derived analytical distribution in (9). The plots visibly show the non-zero probability of idle slots, whereas their exact values are listed in the last row of Table I, for all the simulated users, as well as $N_u = \{10, 12\}$. On the other hand, as shown in the figures, for all the simulated users, the degree distribution of uniform access is always constant. It can be also noted that regardless of the number of users, for the uniform access scheme, the probability of any channel slot being idle is zero.

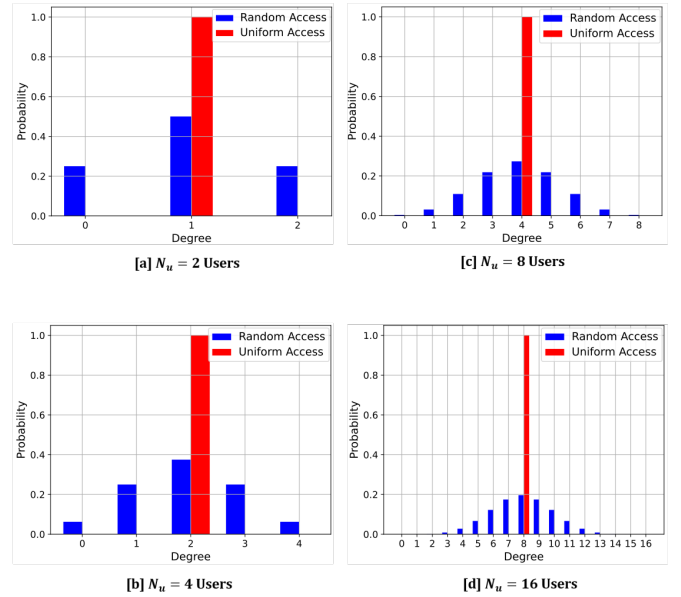


Fig. 3. Node degree distribution comparison of Random and Uniform Channel Access

TABLE I

CAPACITY BOUNDS COMPARISON OF RANDOM ACCESS, UNIFORM ACCESS, AND SPHERE-PACKING BOUNDS, FOR DIFFERENT SPECTRAL EFFICIENCIES, THAT CORRESPOND TO DIFFERENT NUMBER OF USERS, WITH $n_{n_u} = 4320$ SYMBOLS, AND CODE RATE, $r_{n_u} = 1/2$, EACH, ON A CHANNEL WITH $N_s = 8640$ SLOTS

N_u	Single User	2	4	8	10	12	16
η [b/s/Hz]	1	1	2	4	5	6	8
$\left(\frac{E_b}{N_0}\right)_{RA}$ [dB]	0	0.72	2.31	6.06	8.17	10.42	15.21
$\left(\frac{E_b}{N_0}\right)_{UA}$ [dB]	0	0	1.76	5.74	7.92	10.21	15.03
$\left(\frac{E_b}{N_0}\right)_{SPB}$ [dB]	0.69	0.69	2.49	6.59	8.84	11.20	16.17
Δ_{SPB-UA} [dB]	0.69	0.69	0.73	0.85	0.92	0.99	1.13
Δ_{RA-UA} [dB]	0	0.72	0.55	0.32	0.25	0.20	0.17
RA Prob. of empty slots	0	0.25	0.06	3.9e-3	9.7e-4	2.4e-4	1.5e-5

In the previous section, the spectral efficiency of random access, was derived. Equation (15) is solved numerically, for the minimum $\frac{E_b}{N_0}$, required to achieve a spectral efficiency, η . The minimum SNR per bit, $\left(\frac{E_b}{N_0}\right)_{RA}$, of the random access scheme, is listed in the third row of Table I, for the same parameters as in Figure 3, $N_u = \{2, 4, 8, 10, 12, 16\}$ users, and rate- $\frac{1}{2}$ LDPC code. The previous section also derives the attainable spectral efficiency of uniform access, such that (19) gives a closed-form solution, that can be solved mathematically. The minimum SNR per bit, $\left(\frac{E_b}{N_0}\right)_{UA}$, of the uniform access scheme is calculated for the various number of users, and listed in the fourth row in Table I. Moreover, the fifth and sixth rows, respectively show the Sphere-Packing Bound (SPB) [31], and the power efficiency gap between the SPB and the uniform access. Furthermore, the seventh row in the table, lists the gap in the power efficiency between the random access and the uniform access schemes. As shown in the table, this power efficiency gap goes hand in hand with the probability of idle slots.

In light of the above discussion, although random access schemes present themselves as excellent candidates to meet the low-latency requirements, the capacity bounds clearly indicate that uniform access schemes are more power efficient. Consequently, this paper proposes a novel uniform access scheme, dubbed Collision Diversity SCRAM (CoD-SCRAM), to leverage the gap in capacity. Meanwhile, in order to maintain the low-latency, the proposed scheme ensures that the coordination is kept minimal.

IV. LDPC: A BLAST FROM THE PAST

This section constitutes a crucial step in the proposal of the Collision-Diversity SCRAM scheme. It highlights the analogy between the capacity-approaching classical LDPC codes, and the proposed SCRAM algorithm. In essence, it sheds light on the design aspects of powerful LDPC codes, and maps and them to the SCRAM algorithm.

Inspired by BP, the essence of the SCRAM algorithm lies in the flow of soft information on a joint three-layer Tanner graph, that comprises variable nodes, and both SA and LDPC check nodes. Because the graphical structure of the classical LDPC two-layer Tanner graph has a profound impact on the performance of the LDPC code, the graphical features of the three-layer Tanner graph of SCRAM are also provisioned to impact its decoding performance drastically. These features are mainly portrayed in cycles and trapping sets.

A. Impact of Cycles

An (n, k) LDPC code is represented by a Tanner graph that comprises n variable nodes, and $m \geq n - k$ check nodes [32]. The performance of the iterative BP algorithm is optimal provided that the Tanner graph does not include cycles [33]. The presence of short cycles in the Tanner graph hinders the performance of BP and leads to error propagation [34].

On an LDPC Tanner graph, a cycle is defined as a path that starts and terminates at the same node, and goes through a sequence of distinct nodes via their connected edges [33]. A cycle of length L is referred to as an L -cycle. The girth of a Tanner graph is denoted by g , and is defined as the length of the shortest cycle within the graph [35]. A cycle profile is a quantitative analysis of the number of short cycles within a Tanner graph, whose length is less than double the girth [33].

Concerning SCRAM, two sub-definitions of cycles of the three-layer Tanner graph are declared; a local cycle and a global cycle. A local cycle on the SCRAM Tanner graph denotes a cycle that initiates and terminates at a given variable node, that belongs to a certain user, by means of traversing a path between variable nodes and LDPC check nodes that represent the LDPC code of the denoted user. A global cycle on the other hand, is defined as a cycle that initiates and terminates at a variable node, that belongs to a certain user, by means of traversing a path between variable nodes and LDPC check nodes that belong to different users, via trespassing their commonly connected SA check nodes.

The cycle-counting algorithm proposed in [35] yields the cycle profile of classical LDPC codes. In order to obtain the cycle profile of SCRAM, two possible approaches could be followed. The first approach involves the mapping of the SCRAM three-layer Tanner graph to a joint SCRAM parity check matrix, which is then fed to the cycle-counting algorithm in [35], yielding the cycle profile of SCRAM. Alternatively, a thorough analysis of the the SCRAM three-layer Tanner graph lead to the proposal of a cycle-counting algorithm that is specifically tailored for SCRAM. This algorithm focuses on the global cycles of length eight as it was proven by the analysis to constitute a lower bound on the girth of SCRAM.

B. Impact of Trapping Sets

Another important aspect that hinders the performance of LDPC is the Trapping Sets. The concept of trapping sets emerged from the stopping sets that deteriorate the performance of LDPC codes on the Binary Erasure Channel (BEC) [36]. In a nutshell, a stopping set refers to the set of variable nodes, in the Tanner graph of an LDPC code, that are still erased (possess erased bits), after the iterative decoding.

Similar to the stopping sets, the trapping sets, on the Binary Symmetric Channel (BSC), or the AWGN channel, denote the

set of variable nodes that are connected to unsatisfied check nodes, after exhausting the predefined iterations of the iterative decoder [37]. In a similar fashion to BEC, these are the sets that trap the LLRs within the induced subgraph, preventing the decoder from convergence. While the cycles contribute in bouncing the belief (or LLR) of one variable node back to itself, violating the concept of extrinsic information, the presence of trapping sets enhances the weight of the invalid bounced-back beliefs. In other words, the variable nodes become trapped in their own misleading beliefs, causing the iterative decoding to fail, and the error rate curves to saturate.

Although the mapping between the trapping sets on the two-layer Tanner graph of LDPC, and the three-layer Tanner graph of SCRAM, is not straightforward, the analogy still holds. In simple terms, similar to the discussion on local and global cycles, a subgraph on the SCRAM Tanner graph, that involves variable nodes, SA check nodes, and LDPC check nodes, which cause the beliefs to be trapped, could be regarded as a global SCRAM trapping set.

C. Problem Statement, Objective, and Design Guidelines

To sum up, in a similar analogy to BP decoding of classical LDPC codes on a two-layer Tanner graph, the SCRAM mechanism jointly resolves collisions and decodes the LDPC codewords on a hybrid three-layer Tanner graph. The results in [23] depict the drastic outperformance of SCRAM over the sequential state-of-the-art decoders presented in the literature. A glimpse on the theoretical capacity bounds, highlights the superiority of uniform access over the random access schemes, due to the zero probability of idle slots attributed to the uniform access. Consequently, attempting to replace the random access with uniform access within the SCRAM mechanism is provisioned to further improve its performance.

A first intuitive idea is to adopt a uniform Sequential SCRAM mechanism. The key concept is to distribute the modulated symbols of the N_u users, evenly among the N_s slots, such that for $n_s = 1, \dots, N_s$, every SA check node, s_{n_s} , possesses the same degree, $d_{s_{n_s}}$. The simplicity of the sequential access scheme lies in the systematic mapping of the users' symbols, sequentially to the channel slots. In other words, The first user should be assigned the first n_{n_u} slots, to sequentially transmit its n_{n_u} symbols. The second user should then take the next n_{n_u} slots. This process is repeated till all the N_s slots are exhausted. In a similar fashion multiple rounds should be made to accommodate the remaining users. The process is terminated when all the users are accommodated.

A global 8-cycle on the SCRAM three-layer Tanner graph comprises three main constituent components; two connected variable nodes that belong to one user, two connected variable nodes that belong to another user, and two shared SA check nodes. A careful inspection of the sequential uniform access scheme reveals that this access scheme constitutes a rich environment for this typical cycle pattern.

In the sequential uniform access, two or more users fully overlap in a sequential fashion. This means that every variable node within one user set, overlaps with the variable node (or nodes) of the same respective index within the other user (or users) set. As a result, if two variable nodes within one user set are connected by one or more LDPC check nodes, it is guaranteed that their corresponding variable nodes

within the other user (or users) set are also connected. Since the sequential channel access ensures that these connected variable nodes on the different users' sides share the same SA check nodes, the typical 8-cycle pattern is guaranteed. In conclusion, in order to reduce the number of global 8-cycles, the typical cycle pattern has to be disrupted.

In progression, a modified version of the sequential uniform access, dubbed interleaved uniform access is proposed. The key idea is to maintain the uniform degree distribution of the channel slots, while significantly reducing the number of global 8-cycles. The essence of the proposed access scheme lies in the adoption of random interleavers, that break the typical cycle structure of global 8-cycles. This means that while the users are still assigned sequential channel slots, prior to transmission, each user passes its modulated symbols to a random interleaver. The interleaved symbols are then transmitted sequentially over the channel slots. Thus, although similar to the sequential access, two or more users fully overlap over one of the channel subgraphs, the order of their symbols is different. As a result, it is no longer guaranteed that two connected variable nodes on one user set, would collide on the SA slots, with two connected variable nodes on the other user (or users) set.

A thorough investigation of the sequential uniform access and the interleaved uniform access schemes, reveals that both schemes possess common structure of the so-called global trapping sets. In both schemes, each group of users fully overlap on a subset of the channel slots, yielding the overall Tanner graph of the SCRAM system, as multiple disjoint subgraphs. Each of these disjoint subgraphs constitutes a global SCRAM trapping set, which fully traps the beliefs within the subgraph, resembling the definition of conventional trapping sets on LDPC Tanner graphs. Even in the case of the interleaved uniform access, where each user interleaves their symbols before transmission, each group of users is assigned the same set of channel slots as in the case of the sequential access scheme. This means that, each group of users fully overlap on one subgraph, only in a different order of their transmitted symbols.

In the next section, a novel channel access scheme, dubbed Collision Diversity SCRAM (CoD SCRAM), that tackles the problem of global trapping sets within the three-layer Tanner graph, is proposed. The proposed scheme combines the advantages of the previously proposed schemes, while optimizing the global trapping set structure. This means that the proposed CoD SCRAM scheme maintains the uniform degree distribution of the channel slots, just like the sequential and the interleaved access schemes. Moreover, as will be illustrated in the subsequent sections, the proposed scheme possesses less global 8-cycles than the interleaved access scheme, which is provisioned to have far less ones than the sequential access scheme. Furthermore, the proposed scheme tackles the problem of the trapping disjoint subgraphs.

The essence of the proposed CoD SCRAM scheme lies in broadening the spectrum of the joint SCRAM decoder, allowing it to gather reliable beliefs from all nodes within the three-layer Tanner graph. Unlike the sequential and the interleaved access schemes, each user within the proposed access scheme is encouraged to transmit their symbols on

multiple subgraphs. A user with poor conditions, would have their symbols spanning the multiple subgraph, wrecking the chance of a complete set of users being trapped. In other words, the proposed scheme leverages diversity by means of allowing (for the same channel slot degree) the maximum number of users to collide.

V. CoD-SCRAM: UNIFORM INTERLEAVED SCRAM WITH COLLISION DIVERSITY

In compliance with the conventional SCRAM scheme, the proposed Collision Diversity system accommodates N_u users, with n_{n_u} symbols each. The shared channel comprises N_s slots, with n_s denoting the slot index. Moreover, it is assumed that the number of channel slots, N_s , is an integer multiple, $N_{subgraphs}$, of the number of symbols per user, n_{n_u} . This means that the shared access channel can be regarded as $N_{subgraphs}$ subchannels, with n_{n_u} slots each. Unlike the sequential and the interleaved uniform access schemes, where two or more users fully collide on each subgraph, rendering the three-layer Tanner graph as $N_{subgraphs}$ disjoint subgraphs, the Collision Diversity scheme provides a full-span access across all the $N_{subgraphs}$.

Each user, U_{n_u} , hops over the subgraphs in a cyclic fashion at a fixed step size, in order to evenly distribute its n_{n_u} symbols among the $N_{subgraphs}$ subgraphs. Unlike the interleaved uniform access, where the data symbols of each user are being interleaved prior to transmission, in the CoD SCRAM scheme, it is the indices of the channel slots that are actually interleaved. Each set of n_{n_u} channel slots within one subgraph is interleaved separately. This condition ensures that when the users hop over the subgraphs with the interleaved slots, they still spread their symbols equally across the different subgraphs. Moreover, assuming that the number of users, N_u , is an integer multiple of the number of subgraphs, $N_{subgraphs}$, each group of $N_{subgraphs}$ users experience the same interleaved version of the channel slots. The interleaving process changes from one set of $N_{subgraphs}$ users to another.

In order to minimize coordination, the interleaving of the channel slots within each subgraph, can be fulfilled by means of a Linear Feedback Shift Register (LFSR) [38], with a seed that is a function of both the user set index, and the subgraph index. The user set index is denoted by n_{set} , and refers to the index of the set of $N_{subgraphs}$ users that experience the same interleaved version of the channel slots. The total number of user sets, N_{sets} , is thus given by the ratio between the total number of users, N_u , and the number of subgraphs, $N_{subgraphs}$. As a result, the user set index, n_{set} , goes from $n_{set} = 1$ to $n_{set} = N_{sets} = N_u N_{subgraphs}$. The subgraph index, on the other hand, is denoted by n_{sub} , such that $n_{sub} = 1, \dots, N_{subgraphs}$.

For $n_u = 1, \dots, N_u$, each user, U_{n_u} , first calculates the index of the user set, n_{set} , that it belongs to. Because each user set comprises $N_{subgraphs}$ users, the user set index is given by $n_{set} = \lceil \frac{n_u}{N_{subgraphs}} \rceil$. After that, each user, U_{n_u} , activates $N_{subgraphs}$ different LFSRs, each seeded by the user's user set index, n_{set} , and the subgraph index, n_{sub} , of the corresponding subgraph, such that $n_{sub} = 1, \dots, N_{subgraphs}$. For $n_{set} = 1, \dots, N_{sets}$, and $n_{sub} = 1, \dots, N_{subgraphs}$, let $\mathbf{\Pi}^{(n_{set}, n_{sub})} = [\pi_1^{(n_{set}, n_{sub})}, \dots, \pi_{n_{n_u}}^{(n_{set}, n_{sub})}]$, be the vector

of n_{n_u} interleaved indices of subgraph, n_{sub} , and users that belong to user set, n_{set} .

For convenience, it is assumed that for $n_{sub} = 1, \dots, N_{subgraphs}$, the respective interleaver vectors, $\mathbf{\Pi}^{(n_{set}, n_{sub})}$, correspond to the output of the LFSRs, added to a shift value, so that the interleaved indices could directly point to the slot indices, not within the subgraph, but within the total set of N_s channel slots. Thus, while all the LFSRs of the $N_{subgraphs}$ interleavers would output randomized indices between 1 and n_{n_u} , for $n_{sub} = 1, \dots, N_{subgraphs}$, the indices within $\mathbf{\Pi}^{(n_{set}, n_{sub})}$ include a shift by $(n_{sub} - 1) n_{n_u}$.

After interleaving the slots, each of the N_u users has access to $N_{subgraphs}$ interleaved vectors, of the $N_{subgraphs}$ subblocks of the channel slots, with n_{n_u} interleaved slots each. The channel access takes place concurrently for all the users, such that each user hops over the subgraphs in a cyclic fashion, and picks one slot at a time at a fixed step size. Within every user set, each user starts at a different subgraph, picks up a specific slot within the interleaved version of the subgraph, and hops to the next subgraph. When the user exhausts all the subgraphs, it hops back to the first subgraph, and continues with the pickup process.

Within each user set, the first user, U_{n_u} , such that $n_u = (n_{set} - 1) N_{subgraphs} + 1$, starts at the first interleaved subgraph, $\mathbf{\Pi}^{(n_{set}, 1)}$, and picks up the first interleaved slot, $\pi_1^{(n_{set}, 1)}$, to transmit its first symbol. After that, it hops to the second interleaved subgraph, $\mathbf{\Pi}^{(n_{set}, 2)}$, and transmits its second modulated symbol on the second interleaved slot, $\pi_2^{(n_{set}, 2)}$. The user continues hopping till it exhausts all the subgraphs. At this point, the user hops back to the first interleaved subgraph, $\mathbf{\Pi}^{(n_{set}, 1)}$, and picks the interleaved slot, $\pi_{N_{subgraphs}+1}^{(n_{set}, 1)}$, at index $N_{subgraphs} + 1$, to transmit its $N_{subgraphs}$ modulated symbol. The process continues till the user transmits all its n_{n_u} modulated symbols.

The second user within the same set, U_{n_u} , such that $n_u = (n_{set} - 1) N_{subgraphs} + 2$, repeats the same process, except that it starts at the second interleaved subgraph, $\mathbf{\Pi}^{(n_{set}, 2)}$, and picks up the first interleaved slot, $\pi_1^{(n_{set}, 2)}$, to transmit its first modulated symbol. Here again, when the user exhausts all the subgraphs, it hops back to the first interleaved subgraphs, and continues till it transmits all its n_{n_u} modulated symbols.

The same process is repeated in parallel, for all the different N_{sets} sets of users, and all the $N_{subgraphs}$ users per user set. Each user set experiences a different version of the $N_{subgraphs}$ interleaved vectors, based on its user set index, n_{set} , while each user starts at a different interleaved subgraph, $\mathbf{\Pi}^{(n_{set}, n_{sub})}$, based on its user index, n_u . In general terms, for $n_u = 1, \dots, N_u$, the starting interleaved subgraph of user U_{n_u} , is $\mathbf{\Pi}^{(n_{set}, n_{sub})}$, such that $n_{set} = \lceil \frac{n_u}{N_{subgraphs}} \rceil$, and $n_{sub} = \text{mod}(n_u - 1, N_{subgraphs}) + 1$. For $i = 1, \dots, n_{n_u}$, user U_{n_u} sends its i^{th} modulated symbol, on the i^{th} interleaved index, within the interleaved vectors of its current user set, starting at its calculated n_{sub} , and going with incrementing i , in increments of one (with mod operation to go back to first subgraph when all subgraphs are exhausted). Consequently, if $n_s^{(n_u, i)}$ denotes the index of the channel slot, that user U_{n_u} , sends its i^{th} modulated symbols on, for $n_u = 1, \dots, N_u$, and $i = 1, \dots, n_{n_u}$, $n_s^{(n_u, i)}$ is given by

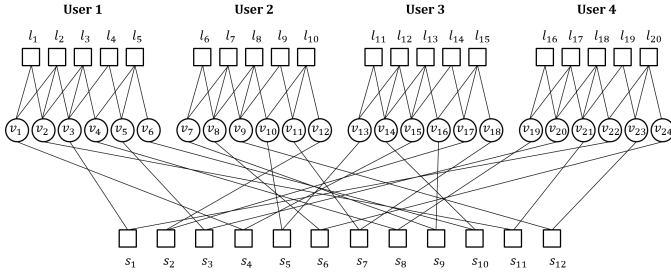


Fig. 4. Interleaved Uniform Access with Collision Diversity example, of a SCRAM system with $N_u = 4$ users, $n_{n_u} = 6$ modulated symbols per user, and $N_s = 12$ SA slots

$$n_s^{(n_u, i)} = \pi_i^{(n_{set}, \text{mod}(n_u + i - 2, N_{subgraphs}) + 1)}, \quad (21)$$

where the R.H.S of (21) corresponds to the i^{th} interleaved index, within the interleaved vector, $\mathbf{\Pi}^{(n_{set}, n_{sub})}$, such that $n_{sub} = \text{mod}(n_u + i - 2, N_{subgraphs}) + 1$, and $n_{set} = \lceil \frac{n_u}{N_{subgraphs}} \rceil$.

The corresponding CoD three-layer Tanner graph can be generated by connecting SA check node, $s_{n_s^{(n_u, i)}}$, where $n_s^{(n_u, i)}$ is calculated as per (21), to variable node, $v_{n_v^{(n_u, i)}}$, such that for $n_u = 1, \dots, N_u$, and $i = 1, \dots, n_{n_u}$, $n_v^{(n_u, i)}$ is given by

$$n_v^{(n_u, i)} = i + (n_u - 1) n_{n_u}. \quad (22)$$

Consider the example in Figure 4, of a CoD SCRAM system with $N_u = 4$ users, and $n_{n_u} = 6$ symbols per user. The shared channel comprises $N_s = 12$ slots, that could be regarded as $N_{subgraphs} = 2$ subgraphs, with $n_{n_u} = 6$ slots each. The total number of user sets is given by $N_{sets} = \frac{N_u}{N_{subgraphs}} = 2$, with $N_{subgraphs} = 2$ users per user set. The user set index, n_{set} , is calculated as $n_{set} = \lceil \frac{n_u}{N_{subgraphs}} \rceil$, such that users U_1 and U_2 belong to $n_{set} = 1$, while users U_3 and U_4 belong to $n_{set} = 2$. Consequently, users U_1 and U_2 generate $N_{subgraphs} = 2$ interleaved vectors, $\mathbf{\Pi}^{(1,1)}$ and $\mathbf{\Pi}^{(1,2)}$, seeded by a function of $n_{set} = 1$ and $n_{sub} = 1$, and 2, respectively. Meanwhile, users U_3 and U_4 generate $N_{subgraphs} = 2$ interleaved vectors, $\mathbf{\Pi}^{(2,1)}$ and $\mathbf{\Pi}^{(2,2)}$, seeded by a function of $n_{set} = 2$ and $n_{sub} = 1$, and 2, respectively.

For the two interleaved instances of the second subgraph, i.e., $\mathbf{\Pi}^{(1,2)}$ and $\mathbf{\Pi}^{(2,2)}$, the output of the LFSRs is shifted by $(n_{sub} - 1) n_{n_u}$, such that $n_{sub} = 2$. This means that for both $n_{set} = 1$ and $n_{set} = 2$, the output of the LFSR at $n_{sub} = 2$, is shifted by six to point directly to the corresponding index within the $N_s = 12$ channel slots.

Let the two interleaved vectors at $n_{set} = 1$, be $\mathbf{\Pi}^{(1,1)} = [4, 6, 1, 5, 3, 2]$ and $\mathbf{\Pi}^{(1,2)} = [9, 11, 12, 8, 7, 10]$, which correspond to $n_{sub} = 1$ and $n_{sub} = 2$, respectively. Similarly, for $n_{sub} = 1$ and $n_{sub} = 2$, let the two interleaved vectors at $n_{set} = 2$, be $\mathbf{\Pi}^{(2,1)} = [5, 3, 4, 1, 2, 6]$ and $\mathbf{\Pi}^{(2,2)} = [8, 10, 11, 9, 12, 7]$, respectively. User U_1 belongs to user set $n_{set} = 1$, and starts at subgraph, $n_{sub} = \text{mod}(n_u - 1, N_{subgraphs}) + 1 = 1$, by picking up the first interleaved slot, $\pi_1^{(1,1)} = 4$, from $\mathbf{\Pi}^{(1,1)}$, to transmit its

first modulated symbol. After that, U_1 picks up the second interleaved slot, $\pi_2^{(1,2)} = 11$, from $\mathbf{\Pi}^{(1,2)}$, to transmit its second modulated symbol. Now that all the subgraphs are exhausted, U_1 goes back to the first subgraph and picks up the third interleaved slot, $\pi_3^{(1,1)} = 1$, from $\mathbf{\Pi}^{(1,1)}$, to transmit its third modulated symbol. U_1 keeps on hopping over the subgraphs till it transmits its six modulated symbols.

Similarly, user U_2 also belongs to user set $n_{set} = 1$, but starts at subgraph, $n_{sub} = 2$, by picking up the first interleaved slot, $\pi_1^{(1,2)} = 9$, from $\mathbf{\Pi}^{(1,2)}$, to transmit its first modulated symbol. User U_2 already exhausts the subgraphs after the first pickup. As a result, for its next hop, U_2 goes back to the first subgraph and picks up the second interleaved slot, $\pi_2^{(1,1)} = 6$, from $\mathbf{\Pi}^{(1,1)}$, to transmit its second modulated symbol. U_2 then continues by picking up the third interleaved slot, $\pi_3^{(1,2)} = 12$, from $\mathbf{\Pi}^{(1,2)}$, to transmit its third modulated symbol, and so on. In a similar fashion, users U_3 and U_4 start at $n_{sub} = 1$ and $n_{sub} = 2$, respectively, at the interleaved vectors, $\mathbf{\Pi}^{(2,1)}$ and $\mathbf{\Pi}^{(2,2)}$, that correspond to $n_{set} = 2$.

Alternatively, (21) could directly compute the slot index of the i^{th} modulated symbol of user U_{n_u} , for $n_u = 1, \dots, N_u$, and $i = 1, \dots, n_{n_u}$. For example, the third modulated symbol of user U_1 , corresponds to $n_u = 1$ and $i = 3$. According to (21), the corresponding slot index, $n_s^{(1,3)}$, is given by $\pi_3^{(n_{set}, 1)}$, such that $n_{set} = 1$ is the user set index of U_1 . Thus, the slot index at which U_1 sends its third modulated symbol is $\pi_3^{(1,1)} = 1$, which corresponds to the third interleaved index, on the first subgraph, of the first interleaving set, $\mathbf{\Pi}^{(1,1)}$. According to (22), the corresponding variable node index, $n_v^{(1,3)}$, of the third modulated symbol of U_1 , is given by $n_v^{(1,3)} = 3$. Therefore, on the three-layer Tanner graph, variable node v_3 , is connected to SA check node s_1 .

Figure 5 shows the flowchart of the proposed CoD SCRAM, at an arbitrary user terminal, U_{n_u} . Based on the assigned user ID, n_u , the user calculates the index of the user set, n_{set} , to which it belongs. The user then loops over the indices, n_{sub} , of the $N_{subgraphs}$ blocks of channel slots. For $n_{sub} = 1, \dots, N_{subgraphs}$, the user generates $N_{subgraphs}$ interleaved vectors, $\mathbf{\Pi}^{(n_{set}, n_{sub})}$, generated by LFSRs, that are seeded by a function of both n_{set} and n_{sub} , and shifted to match the index of the slots within the N_s slots. After that, the user loops over its n_{n_u} symbols, and for every symbol index i , such that $i = 1, \dots, n_{n_u}$, U_{n_u} , calculates the corresponding slot index, $n_s^{(n_u, i)}$. The algorithm halts when the corresponding slots of all the n_{n_u} symbols are calculated.

VI. CYCLE PROFILE OF COD-SCRAM

In this section, the cycle profile of the proposed CoD SCRAM, is to be analyzed. The analysis is carried out in two parallel directions. First, the three-layer Tanner graph of the collision diversity SCRAM scheme is mapped to a two-dimensional hybrid matrix, which is then fed to the cycle counting algorithm in [35], yielding the cycle-profile of the proposed scheme. Meanwhile, the global 8-cycles counter algorithm, quantifies the number of added global 8-cycles, that result from the adoption of the collision diversity scheme.

In order to have a full picture, the analysis of the SCRAM systems with sequential, interleaved, and random access

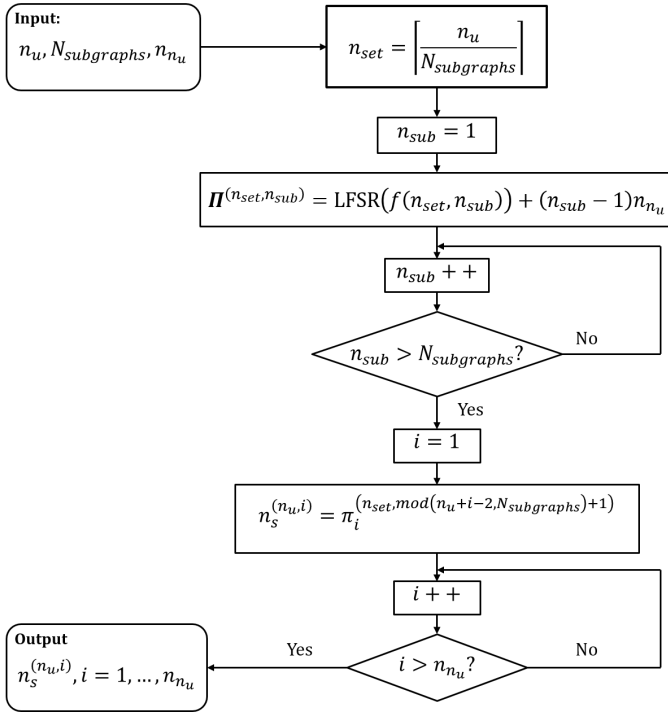


Fig. 5. Flowchart of Interleaved Uniform Access SCRAM with Collision Diversity, on each user terminal, U_{n_u} , in the uplink scenario

schemes is included for convenience. The SCRAM system accommodates $N_u = 4$ user, with $n_{n_u} = 4320$ symbols each. The adopted LDPC encoders are assumed to be identical for all the four users, and correspond to the (4320, 2160) code, taken from the DVB-NGH standard [39]. The shared access channel comprises $N_s = 8640$ slots, which can be regarded as $N_{subgraphs} = 2$ subgraphs, with $n_{n_u} = 4320$ slots each.

The cycle profile of the SCRAM systems with the different access methods, along with the number of global 8-cycles is depicted in Table II. The first row shows the cycle profile of the (4320, 2160) DVB-NGH [39] LDPC code. The second row shows the cycle profile of the proposed CoD SCRAM, along with its global 8-cycle count. The results of the sequential, interleaved, and random access schemes, are depicted in the third, fourth, and fifth rows, respectively.

For all the access schemes, the number of 6-cycles from

TABLE II
CYCLE PROFILE OF SCRAM, WITH $N_u = 4$ USERS, ADOPTING THE (4320, 2160) DVB-NGH LDPC CODE, WITH INTERLEAVED UNIFORM ACCESS WITH COLLISION DIVERSITY, ON A CHANNEL WITH $N_s = 8640$ SLOTS

	Cycle Profile (LDPC)		Global 8-Cycles	Cycle Profile (SCRAM)	
	C_6	C_8		C_6	C_8
DVB NGH LDPC	31200	1558340			
Collision Diversity			482	124800	6233842
Sequential			138224	124800	6371584
Interleaved			1002	124800	6234362
Random Access			725	124800	6234085

the cycle profile is four times that of pure LDPC. This proves that all the 6-cycles in the three-layer Tanner graph of the respective SCRAM system are local LDPC cycles, and that the schemes do not add global cycles of length six. Concerning the 8-cycles, for all the access methods, the total number of 8-cycles from the cycle profile corresponds to four times that of LDPC, in addition to the number of global 8-cycles, obtained from the global 8-cycles counter. As a result, the validity of the algorithmic global 8-cycles counter is verified.

As shown in the table, the CoD scheme possesses the least number of global 8-cycles, in comparison to the other access schemes. The small number of global 8-cycles, along with its ability to unlock the trapping sets, are provisioned to let the CoD scheme outperform the other tackled access schemes.

VII. RESULTS

This section is dedicated to evaluating the PER performance of the proposed CoD SCRAM scheme, in comparison to the sequential, interleaved, and random access SCRAM schemes. For all the access schemes, the system incorporates $N_u = 4$ users. Each user adopts a (4320, 2160), rate $1/2$, LDPC code, taken from the DVB-NGH standard [39]. The $n_{n_u} = 4320$ encoded bits of each user are first BPSK modulated, and then equalized by the estimated magnitude of the Rayleigh fading coefficients, assuming perfect CSI at the transmitter. The shared access channel comprises $N_s = 8640$ frequency subcarriers. The superimposed received symbols are perturbed by complex AWGN of zero mean, and variance N_0 . At the receiver side, the joint SCRAM decoder runs 50 decoding iterations on the three-layer Tanner graph.

Figure 6 shows the PER performance, of the proposed CoD SCRAM scheme, simulated vs. $\frac{E_b}{N_0}$. The figure also depicts the results of the sequential, interleaved, and the random access SCRAM schemes, along with the capacity bounds of both uniform and random access. As provisioned, the proposed collision diversity scheme drastically outperforms the sequential, interleaved, and the random access schemes.

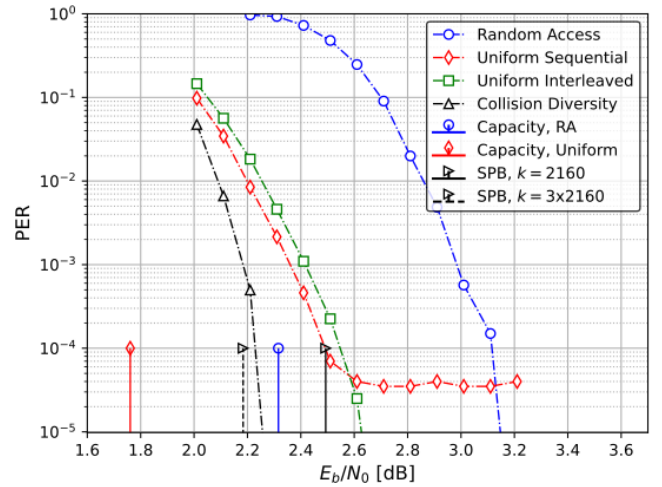


Fig. 6. PER comparison of Interleaved Uniform Access with Collision Diversity, Interleaved Uniform Access, Sequential Uniform Access, and Random Access vs. SPB, of SCRAM with $N_u = 4$ Users, $N_s = 8640$ slots, and (4320, 2160) NGH LDPC, over Rayleigh fading and pre-equalization at the transmitter side, simulated for a sample size of 10^5 packets per user

As depicted in the figure, at the PER of 10^{-3} and 10^{-4} , the CoD scheme outperforms the interleaved uniform access by approximately 0.23 dB and 0.32 dB, respectively. The collision diversity scheme is also 0.096 dB better than the capacity bounds of random access.

In comparison to the capacity of uniform access, the CoD scheme is yet 0.46 dB short of the ultimate capacity bound. The reason behind this capacity gap, is the relatively short information block length (2160), of the adopted LDPC code. This in fact leads to the inclusion of the Sphere-Packing Bound (SPB) [31], [40], which is a more realistic bound, that takes the information block length into consideration. The figure also shows the SPB calculated for $k = 2160$, and $k = 3 \times 2160$, plotted in a solid and a dashed line, respectively. As shown in the figure, the proposed CoD SCRAM is superior to the SPB calculated at $k = 2160$ by approximately 0.25 dB. The noted outperformance of the proposed CoD SCRAM can be justified by a virtual enhancement in the effective block length.

More specifically, a CoD SCRAM system with N_u users over $N_s = N_{subgraphs} \times n$ channel slots, ensures that each user collides with $(N_{subgraphs} - 1)(N_u N_{subgraphs})$ users. Consequently, by adopting the law of large numbers [41], the effective information block length is enhanced by a factor of approximately $((N_{subgraphs} - 1)(N_u N_{subgraphs}) + 1)$. For the simulations presented herein, with $N_u = 4$ users, $N_s = 2n$, the number of subgraphs is given by $N_{subgraphs} = 2$. Consequently, the effective block length is given by $3k$. For this reason, Figure 6 shows the SPB calculated at block length of $3k$. As shown in the figure, the performance of the CoD SCRAM is only approximately 0.056 dB away from that SPB.

In order to highlight the essence of the proposed CoD SCRAM scheme, the simulations are extended to higher number of users, at the same channel load. In this simulation apparatus, the objective is to assess the impact of the proposed CoD scheme on the effective information block length. As a result, for the adopted simulations, a target channel load, D , is set and kept fixed. Meanwhile, the simulations are carried out for various number of users, N_u . In order to keep the channel load fixed, going for higher number of users corresponds to increasing the number of channel slots, N_s , in order to meet the target channel load.

Figure 7 depicts the PER performance of the proposed CoD SCRAM system at a target channel load of $D = 1$. The system is simulated for $N_u = \{4, 6, 8, 10\}$ users. Thus, the number of adopted channel slots is given by $N_s = \{2n, 3n, 4n, 5n\}$, respectively, where n is the length of the LDPC codeword at the output of the LDPC encoder. This means that for the CoD scheme, the number of subgraphs is given by $N_{subgraphs} = \{2, 3, 4, 5\}$, respectively. Similar to the previous simulation, the users adopt the rate $1/2$, (4320, 2160) LDPC code from the DVB NGH standard [39].

Figure 7 also depicts the theoretical capacity bounds. The leftmost bound corresponds to the ultimate capacity bound, while the rightmost bound represents the SPB calculated at information block length $k = 2160$. Meanwhile, the SPB at the enhanced length of $3k$, $5k$, $7k$, and $9k$, that corresponds to $N_u = 4, 6, 8$, and 10 users, respectively, is calculated and plotted for convenience. The figure sheds the light on numerous observations. First, although all the plotted PER curves correspond to a fixed channel load, D , going for

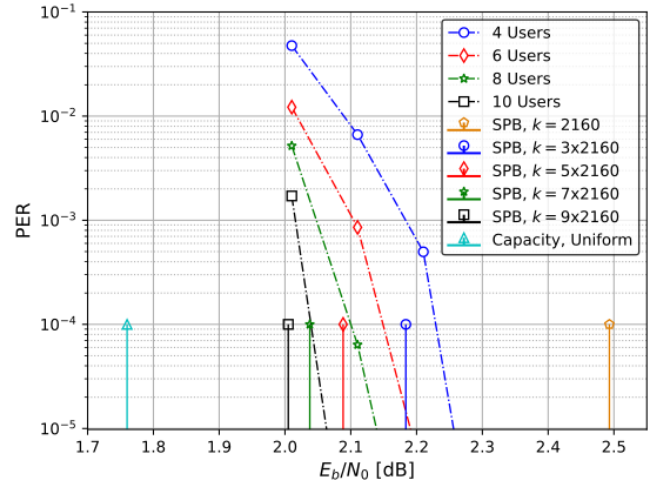


Fig. 7. PER comparison of Interleaved Uniform Access with Collision Diversity, for $N_u = \{4, 6, 8, 10\}$ users, channel load of 1, and (4320, 2160) NGH LDPC, over Rayleigh fading and pre-equalization at the transmitter side, simulated for a sample size of 10^5 packets per user, plotted against SPB at different information block lengths

higher number of users leads to further improvement in the PER performance. For example, at the PER of 10^{-3} , the performance of the proposed CoD SCRAM system with six, eight, and ten users, is superior to that of the four users by approximately 0.08 dB, 0.14 dB, and 0.17 dB, respectively. In comparison to the ultimate capacity bound, the figure shows that at the PER of 10^{-4} , the gap between the performance of the four, six, eight, and ten users, to the ultimate capacity bound, reduces to approximately 0.46 dB, 0.38 dB, 0.34 dB, and 0.27 dB, respectively.

In comparison to the SPB, the figure shows that all the plotted curves are superior to the SPB, calculated at $k = 2160$. As shown in the figure, at the PER of 10^{-4} , the CoD SCRAM system with $N_u = 4, 6, 8$, and 10 users outperforms the SPB at $k = 2160$ by approximately 0.27 dB, 0.35 dB, 0.39 dB, and 0.46 dB respectively. As a result, not only does the proposed CoD improve the effective information block length, but also accommodating higher number of users leads to a better utilization of the granted inherent coordination that reflects on the respective PER performance.

Finally, in order to assess the quantification of the effective information block length enhancement, for the CoD systems with $N_u = 4, 6, 8$, and 10 users, and $N_{subgraphs} = 2, 3, 4$, and 5 , respectively, the SPB is calculated at a block length of $3k$, $5k$, $7k$, and $9k$, respectively, where $k = 2160$ is the information block length of the underlying LDPC code. By comparing the PER curves to the respective bounds, it can be shown that the gap is subtle. For instance, at the PER of 10^{-4} , the gap between the PER curves of the proposed CoD system with $N_u = 4, 6, 8$, and 10 users, and the SPB bounds at a block length of $3k$, $5k$, $7k$, and $9k$, is approximately 0.04 dB, 0.06 dB, 0.07 dB, and 0.025 dB, respectively.

VIII. CONCLUSIONS

In this paper, a novel Non-Orthogonal Multiple Access (NOMA)-based approach dubbed Collision Diversity (CoD) SCRAM is proposed. The proposed CoD scheme is regarded

as an enhancement of the conventional Slotted Coded Random Access Multiplexing (SCRAM) mechanism. The essence of SCRAM lies in its ability to jointly resolve collisions and decodes the Low Density Parity Check (LDPC) codewords, in a similar analogy to Belief Propagation (BP) on a joint three-layer Tanner graph. The proposed CoD SCRAM is pillared on three main terminologies. First, it adopts an information-theoretic approach in order to maximize the attainable Spectral Efficiency. Secondly, it utilizes the analogy between the two-layer Tanner graph of classical LDPC codes, and the three-layer Tanner graph of SCRAM, in order to adopt the well-established design tools of powerful LDPC codes to enhance the graphical structure of the SCRAM three-layer Tanner graph. Finally, the proposed CoD SCRAM leverages the collisions among the transmitted packets in order to enhance the respective information block length.

REFERENCES

- [1] S. Jere, Y. Song, Y. Yi, and L. Liu, "Distributed learning meets 6G: A communication and computing perspective," *IEEE Wireless Communications*, vol. 30, no. 1, pp. 112–117, 2023.
- [2] M. S. Akbar, Z. Hussain, Q. Z. Sheng, and S. Mukhopadhyay, "6G survey on challenges, requirements, applications, key enabling technologies, use cases, ai integration issues and security aspects," *arXiv preprint arXiv:2206.00868*, 2022.
- [3] V.-L. Nguyen, R.-H. Hwang, P.-C. Lin, A. Vyas, and V.-T. Nguyen, "Towards the age of intelligent vehicular networks for connected and autonomous vehicles in 6G," *IEEE Network*, 2022.
- [4] S. Mihai, M. Yaqoob, D. V. Hung, W. Davis, P. Towakel, M. Raza, M. Karamanoglu, B. Barn, D. Shetve, R. V. Prasad *et al.*, "Digital twins: a survey on enabling technologies, challenges, trends and future prospects," *IEEE Communications Surveys & Tutorials*, 2022.
- [5] W. Jiang, B. Han, M. A. Habibi, and H. D. Schotten, "The road towards 6G: A comprehensive survey," *IEEE Open Journal of the Communications Society*, vol. 2, pp. 334–366, 2021.
- [6] Z. Ding, M. Peng, and H. V. Poor, "Cooperative non-orthogonal multiple access in 5G systems," *IEEE Communications Letters*, vol. 19, no. 8, pp. 1462–1465, 2015.
- [7] S. Srivastava and P. P. Dash, "Non-orthogonal multiple access: Procession towards B5G and 6G," in *2021 IEEE 2nd International Conference on Applied Electromagnetics, Signal Processing, & Communication (AESPC)*. IEEE, 2021, pp. 1–4.
- [8] O. Maraqa, A. S. Rajasekaran, S. Al-Ahmadi, H. Yanikomeroğlu, and S. M. Sait, "A survey of rate-optimal power domain NOMA with enabling technologies of future wireless networks," *IEEE Communications Surveys & Tutorials*, vol. 22, no. 4, pp. 2192–2235, 2020.
- [9] A. Jehan and M. Zeeshan, "Comparative performance analysis of code-domain NOMA and power-domain NOMA," in *2022 16th International Conference on Ubiquitous Information Management and Communication (IMCOM)*. IEEE, 2022, pp. 1–6.
- [10] Z. Liu and L.-L. Yang, "Sparse or dense: A comparative study of code-domain NOMA systems," *IEEE Transactions on Wireless Communications*, vol. 20, no. 8, pp. 4768–4780, 2021.
- [11] S. Chen, B. Ren, Q. Gao, S. Kang, S. Sun, and K. Niu, "Pattern division multiple access—a novel nonorthogonal multiple access for fifth-generation radio networks," *IEEE Transactions on Vehicular Technology*, vol. 66, no. 4, pp. 3185–3196, 2016.
- [12] H. Nikopour and H. Baligh, "Sparse code multiple access," in *2013 IEEE 24th Annual International Symposium on Personal, Indoor, and Mobile Radio Communications (PIMRC)*. IEEE, 2013, pp. 332–336.
- [13] R. De Gaudenzi, O. del Río Herrero, S. Cioni, and A. Mengali, "Random access versus multiple access," *Multiple Access Techniques for 5G Wireless Networks and Beyond*, pp. 535–584, 2019.
- [14] R. Hoshyar, F. P. Wathan, and R. Tafazolli, "Novel low-density signature for synchronous CDMA systems over AWGN channel," *IEEE Transactions on Signal Processing*, vol. 56, no. 4, pp. 1616–1626, 2008.
- [15] H.-A. Loeliger, "An introduction to factor graphs," *IEEE Signal Processing Magazine*, vol. 21, no. 1, pp. 28–41, 2004.
- [16] S. D. Sosnin, G. Xiong, D. Chatterjee, and Y. Kwak, "Non-orthogonal multiple access with low code rate spreading and short sequence based spreading," in *2017 IEEE 86th Vehicular Technology Conference (VTC-Fall)*. IEEE, 2017, pp. 1–5.
- [17] L. Dai, B. Wang, Z. Ding, Z. Wang, S. Chen, and L. Hanzo, "A survey of non-orthogonal multiple access for 5G," *IEEE communications surveys & tutorials*, vol. 20, no. 3, pp. 2294–2323, 2018.
- [18] L. Ping, L. Liu, K. Wu, and W. K. Leung, "Interleave division multiple-access," *IEEE transactions on wireless communications*, vol. 5, no. 4, pp. 938–947, 2006.
- [19] N. Iswarya and L. Jayashree, "A survey on successive interference cancellation schemes in non-orthogonal multiple access for future radio access," *Wireless Personal Communications*, vol. 120, no. 2, pp. 1057–1078, 2021.
- [20] P. H. Tan and L. K. Rasmussen, "Belief propagation for coded multiuser detection," in *2006 IEEE International Symposium on Information Theory*. IEEE, 2006, pp. 1919–1923.
- [21] X. Meng, Y. Wu, Y. Chen, and M. Cheng, "Low complexity receiver for uplink scma system via expectation propagation," in *2017 IEEE wireless communications and networking conference (WCNC)*. IEEE, 2017, pp. 1–5.
- [22] B. Ren, X. Yue, W. Tang, Y. Wang, S. Kang, X. Dai, and S. Sun, "Advanced IDD receiver for PDMA uplink system," in *2016 IEEE/CIC International Conference on Communications in China (ICCC)*. IEEE, 2016, pp. 1–6.
- [23] S. Nafie, J. Robert, and A. Heuberger, "SCRAM: A novel approach for reliable ultra-low latency m2m applications," in *2018 IEEE 88th Vehicular Technology Conference (VTC-Fall)*. IEEE, 2018, pp. 1–5.
- [24] R. Gallager, "Low-density parity-check codes," *IRE Transactions on information theory*, vol. 8, no. 1, pp. 21–28, 1962.
- [25] A. Munari, M. Heindlmaier, G. Liva, and M. Berlioli, "The throughput of slotted ALOHA with diversity," in *Communication, Control, and Computing (Allerton), 2013 51st Annual Allerton Conference on*. IEEE, 2013, pp. 698–706.
- [26] D. J. MacKay and R. M. Neal, "Near shannon limit performance of low density parity check codes," *Electronics letters*, vol. 33, no. 6, pp. 457–458, 1997.
- [27] R. Tanner, "A recursive approach to low complexity codes," *IEEE Transactions on information theory*, vol. 27, no. 5, pp. 533–547, 1981.
- [28] E. Casini, R. De Gaudenzi, and O. D. R. Herrero, "Contention resolution diversity slotted ALOHA (CRDSA): An enhanced random access scheme for satellite access packet networks," *IEEE Transactions on Wireless Communications*, vol. 6, no. 4, 2007.
- [29] P. M. Altham, "Two generalizations of the binomial distribution," *Journal of the Royal Statistical Society Series C: Applied Statistics*, vol. 27, no. 2, pp. 162–167, 1978.
- [30] J. G. Proakis, *Digital communications*. McGraw-Hill, Higher Education, 2008.
- [31] C. E. Shannon, R. G. Gallager, and E. R. Berlekamp, "Lower bounds to error probability for coding on discrete memoryless channels. i," *Information and Control*, vol. 10, no. 1, pp. 65–103, 1967.
- [32] S. J. Johnson, "Introducing low-density parity-check codes," *University of Newcastle, Australia*, vol. 1, p. 2006, 2006.
- [33] M. Karimi and A. H. Banihashemi, "Message-passing algorithms for counting short cycles in a graph," *IEEE Transactions on Communications*, vol. 61, no. 2, pp. 485–495, 2012.
- [34] X. Xiao, B. Vasić, S. Lin, K. Abdel-Ghaffar, and W. E. Ryan, "Reed-solomon based quasi-cyclic LDPC codes: Designs, girth, cycle structure, and reduction of short cycles," *IEEE Transactions on Communications*, vol. 67, no. 8, pp. 5275–5286, 2019.
- [35] J. Li, S. Lin, and K. Abdel-Ghaffar, "Improved message-passing algorithm for counting short cycles in bipartite graphs," in *2015 IEEE International Symposium on Information Theory (ISIT)*. IEEE, 2015, pp. 416–420.
- [36] Y. Hashemi and A. H. Banihashemi, "On characterization and efficient exhaustive search of elementary trapping sets of variable-regular LDPC codes," *IEEE Communications Letters*, vol. 19, no. 3, pp. 323–326, 2015.
- [37] M. Karimi and A. H. Banihashemi, "Efficient algorithm for finding dominant trapping sets of LDPC codes," *IEEE Transactions on Information Theory*, vol. 58, no. 11, pp. 6942–6958, 2012.
- [38] L.-T. Wang and E. J. McCluskey, "Linear feedback shift register design using cyclic codes," *IEEE Transactions on Computers*, vol. 37, no. 10, pp. 1302–1306, 1988.
- [39] D. Gomez-Barquero, C. Douillard, P. Moss, and V. Mignone, "DVB-NGH: The next generation of digital broadcast services to handheld devices," *IEEE Transactions on Broadcasting*, vol. 60, no. 2, pp. 246–257, 2014.
- [40] S. Dolinar, D. Divsalar, and F. Pollara, "Code performance as a function of block size," *TMO progress report*, vol. 42, no. 133, 1998.
- [41] K. Yao and J. Gao, "Law of large numbers for uncertain random variables," *IEEE Transactions on Fuzzy Systems*, vol. 24, no. 3, pp. 615–621, 2015.